Carbohydrate Polymers 245 (2020) 116526

Contents lists available at ScienceDirect

Carbohydrate Polymers

journal homepage: www.elsevier.com/locate/carbpol

Structure-activity relationship of Citrus segment membrane RG-I pectin against Galectin-3: The galactan is not the only important factor

Dongmei Wu[a], Jiaqi Zheng[a], Weiwei Hu[a], Xiaoliang Zheng[d], Qiaojun He[e], Robert J. Linhardt[f], Xingqian Ye[a,b,c], Shiguo Chen[a,b,c,*]

[a] College of Biosystems Engineering and Food Science, National-Local Joint Engineering Laboratory of Intelligent Food Technology and Equipment, Zhejiang Key Laboratory for Agro-Food Processing, Integrated Research Base of Southern Fruit and Vegetable Preservation Technology, Zhejiang International Scientific and Technological Cooperation Base of Health Food Manufacturing and Quality Control, Zhejiang University, Hangzhou 310058, China
[b] Fuli Institute of Food Science, Zhejiang University, Hangzhou 310058, China
[c] Ningbo Research Institute, Zhejiang University, Ningbo 315100, China
[d] Center for Molecular Medicine, Zhejiang Academy of Medical Sciences, Hangzhou 310013, China
[e] Institute of Pharmacology & Toxicology, College of Pharmaceutical Sciences, Zhejiang University, Hangzhou 310058, China
[f] Center for Biotechnology and Interdisciplinary Studies, Rensselaer Polytechnic Institute, Troy, New York 12180, United States

ARTICLE INFO

Keywords:
Polysaccharide
RG-I regions
Citrus segment membrane
Carbohydrate active enzymes
Galectin-3 inhibitor
SEC-MALLS

ABSTRACT

Rhamnogalacturonan I (RG-I) pectin are regarded as strong galectin-3 (Gal-3) antagonist because of galactan sidechains. The present study focused on discussing the effects of more structural regions in pectin on the anti-Gal-3 activity. The water-soluble pectin (WSP) recovered from citrus canning processing water was categorized as RG-I pectin. The controlled enzymatic hydrolysis was employed to sequentially remove the α-1,5-arabinan, homogalaturonan and β-1,4-galactan in WSP. The Gal-3-binding affinity KD (kd/ka) of WSP and debranched pectins were calculated to be 0.32 μM, 0.48 μM, 0.56 μM and 1.93 μM. Moreover, based on the more sensitive cell line (MCF-7) model, the IC_{30} value of WSP was lower than these of modified pectins, indicating decreased anti-Gal-3 activity. Our results suggested that the total amount of neutral sugar sidechains, the length of arabinan and cooperation between HG and RG-I played important roles in the anti-Gal-3 activity of WSP, not the Gal/Ara ratio or RG-I/HG ratio. These results provided a new insight into structure-activity relationship of citrus segment membrane RG-I as a galectin-3 antagonist and a new functional food.

1. Introduction

Cancer is one of the biggest health problems with global deaths reaching 9.6 million (WHO 2019). Galectin-3, a β-galactoside binding protein, has been regarded as a "culprit molecule" promoting the development of cancers by accelerating the proliferation, adhesion, metastasis and inhibiting the cell apoptosis (Nguyen et al., 2018; Rajput et al., 2016). The expression of Gal-3 differs in various cell types, but the immune-cells and collagen-producing cells seem to be the primary sources of Gal-3 (Suthahar et al., 2018). Gal-3 is up-regulated in many cancers including colorectal, breast and lung cancer (Jiang, Dang, Gong, & Guo, 2019; Newlaczyl & Yu, 2011). The biological properties of Gal-3 are associated with its binding activity, which is due to the interaction of several glycoconjugates with its conserved carbohydrate-recognition domain (CRD) (Laaf, Bojarova, Elling, & Kren, 2019).

Pectin, a plant cell wall polysaccharide, consist predominantly of homogalacturonans (HG), a few rhamnogalacturonan I (RG-I) and a minor rhamnogalacturonan II (RG-II) fraction (Yapo, Wathelet, & Paquot, 2007; Voragen, Coenen, Verhoef, & Schols, 2009; Yapo, Lerouge, Thibault, & Ralet, 2007, 2011). RG-I is viewed as one of the structural components containing the highest rhamnose content ramified in pectin, consisting of repeating [→2)-α-L-Rhap-(1→4)-α-D-GalpA-(1→] units, where a portion of the rhamnose residues are substituted with varying neutral and branched sugar chains, including linear or branched α-(1→5)-arabinan, linear β-(1→4)-galactan, branched β-(1→3,6)-galactan and arabinogalactan (Liu et al., 2018; Maxwell, Belshaw, Waldron, & Morris, 2012; Mohnen, 2008; Ridley, O'Neil, & Mohnen, 2001). Due to the high-temperature and acid extraction method for commercial pectin, RG-I usually exists in agro-industrial by-products after the extraction process (Jiang & Du, 2017; Mao et al., 2020; Pi, Liu, Guo, Guo, & Meng, 2019; Yan et al., 2018), with much more amount than HG regions (Khodaei & Karboune, 2018). Recently, many RG-Is

* Corresponding author at: Hangzhou 310029, China.
E-mail address: chenshiguo210@163.com (S. Chen).

https://doi.org/10.1016/j.carbpol.2020.116526
Received 10 December 2019; Received in revised form 27 May 2020; Accepted 28 May 2020
Available online 05 June 2020
0144-8617/

from fruits and vegetables have been reported to possess excellent anti-Gal-3 activity, such as pumpkin RG-I, citrus peel RG-I, and ginseng RG-I (Wu et al., 2020; Xue et al., 2019; Zhao et al., 2017; Zhang, Lan et al., 2016; Gao et al., 2013). Thus, the novel RG-I pectin is a promising galectin-3 antagonist. Published studies have also revealed that ginseng pectins and chemically modified citrus pectin with different structure exhibited various effects on galectin-3 action, and the short β-1,4 galactan side chains in RG-I play important roles (Zhang, Lan et al., 2016; Gao et al., 2013). However, most of these studies focus on the binding affinity of natural pectic polymers or degraded oligomers. No systematic evaluation of the specific structural region required for anti-Gal-3 activity has been carried out. Such an evaluation requires a modification method that can target the removing specific regions of pectin instead of its random and violent chemical degradation.

Enzyme digestion is an environment-friendly and green approach to achieve mild modification. Different carbohydrate active enzymes can remove targeted sugar chains without any changes in the other domains of pectin (Oosterveld, Pol, Beldman, & Voragen, 2001; Zheng & Mort, 2008). Hence, enzyme catalyzed modification is a preferred method for studying the structure-function relationship of RG-I pectin.

In this study we obtained citrus segment membrane RG-I pectin, the water-soluble pectin (WSP) from citrus canning processing water. The hypothesis was that WSP can antagonize Gal-3 and all of the side chain structures contribute to its anti-Gal-3 activity. The aim of this study is to determine the anti-Gal-3 bioactivity of WSP and discuss the structure-functionality relationship. Three enzymes were used to partly remove the arabinan, homogalacturonan and galactan. We then analyzed the structural changes between WSP and debranched pectin samples to assess their ability to antagonize Gal-3 and determine the important bioactive structural factors. This study is significant, as it should lead to the development of novel Gal-3 antagonists and safe food additives from this natural product and also provide for the potential valorization of a citrus derived agriculture industry waste.

2. Material and methods

2.1. Material

The basic pectin source was collected from citrus fruit canning factories (Ningbo, China). Endo-1,5-α-arabinanase (EC 3.2.1.99, 400 U), endo-polygalacturonase (EC 3.2.1.15, 5000 U), endo-1,4-β-galactanase (EC 3.2.1.89, 1000 U) were purchased from Megazyme International Ireland Ltd. (Wicklow, Ireland). Modified citrus pectin (MCP) was purchased from EcoNugenics (Santa Rosa, CA, USA). Monosaccharide standards, 1-phenyl-3-methyl-5-pyrazolone (PMP) and D_2O were all purchased from Sigma-Aldrich (Shanghai, China). All other chemicals were analytical grade and purchased from Aladdin Co. (Shanghai, China).

2.2. Preparation of WSP and enzymatic modification

The crude pectin was recovered from alkaline water during the citrus segment membrane removal process from fruit canning factories (Chen et al., 2017). The basic processing water underwent a two-step filtration using 200 and 400 meshes filters, neutralization in a pH adjusted reactor, vacuum concentration at 70 °C, and precipitation using ethanol. The precipitates were recovered by alcohol washing and oven-dried at 55 °C for 24 h. The dried pectin powder was dissolved in distilled water (0.5 *g*/100 mL) followed by gentle heating (60 °C, stirring at 600 rpm for 40 min), centrifugation (8000 rpm, 10 min) to obtain the original sample, water-soluble pectin (WSP), and finally freeze-dried.

The method for enzyme-modification of WSP is shown in Fig. 1. WSP (200 mg) was re-dissolved in 0.1 M citric acid-sodium acetate buffer with a final concentration of 2 mg mL^{-1} and subjected to sequential enzymatic hydrolysis by endo-1,5-α-arabinanase (0.2 U mL^{-1} at 40 °C for 48 h, pH 4.0), endo-polygalacturonase (0.05 U mL^{-1} at 40 °C for 72 h, pH 5.5) and endo-1,4-β-galactanase (0.05 U mL^{-1} at 40 °C for 24 h, pH 4.0) under gentle stirring (150 rpm). The resultant hydrolysates were heated at 90 °C for 5 min for terminating enzymatic activity and then, dialyzed (MWCO 10 kDa) against deionized water for three days, and freeze-dried. EP-1 referred to WSP debranched by endo-1,5-α-arabinanase; EP-2 was modified EP-1 treated by endo-polygalacturonase; EP-3 was endo-1,4-β-galactanase-modified EP-2.

2.3. Molecular weight determination of SEC-MALLS

The homogeneity and relative molecular weight of WSP and enzyme-treated pectins were determined using high-performance (HP) size exclusion chromatography (SEC) (on a OHpak SB-G guard column, SB-806 HQ and SB-804 HQ column, 7.8 × 300 mm, Shodex, Japan), and detected with a multi-angle laser light scattering (DAWN HELEOS II, Wyatt Technology, USA), by viscometry (ViscoStar™ III, Wyatt Technology, USA) and by refractive index (SEC-MALLS-VISC-RI) at 25 °C, according to Wei et al., 2019. Samples were dispersed directly in purified water (5 mg mL^{-1}) and filtered through a 0.22 μm filter membrane twice. Solution (50 μL) was injected through a sample loop and the running time was 50 min. The mobile phase was 0.15 M NaCl solution containing 0.02 % NaN3 (pH 7.0) with a flow rate of 0.5 mL min1. Data analysis was performed using ASTRA software, version 7.1.2 (Wyatt Technology).

2.4. Monosaccharide analysis

The monosaccharide composition of every pectic sample was analyzed after derivatization with 1-phenyl-3-methyl-5-pyrazolone (PMP) using high performance liquid chromatography (HPLC) on a Waters e2695 (Waters, US) equipped with a Zorbax Eclipse XDB-C18 column (250 mm × 4.6 mm, 5 μm, Agilent, USA) and detected using a 2489 UV/Vis Detector (Waters, US) at 250 nm as described by Zhang et al., 2018. Briefly, 2 M trifluoroacetic acid (TFA) was first employed to hydrolyze the pectin samples (2 mg) at 110 °C for 8 h in a sealed ampoule and then evaporated with methanol under nitrogen blower to completely remove TFA. Pre-column derivatization was performed using PMP solution (0.5 M, in methanol) at 70 °C for 30 min. Finally, chloroform was used to extract excess reagent three-times. The supernatant was filtered through a 0.22 μm nylon membrane and 10 μL of the resulting solution was injected for analysis. The mobile phases were: solvent A, potassium phosphate buffer (0.05 M, pH 6.9) with 15 % acetonitrile, and solvent B, the same buffer with 40 % acetonitrile.

2.5. ^1H NMR analysis and FT-IR spectroscopy

NMR spectroscopy was performed on pectins (10 − 15 mg) dissolved in 0.5 mL of D_2O (99.96 %) that had been lyophilized twice to replace exchangeable protons (Li et al., 2019) before final dissolution in 0.5 mL D_2O. ^1H NMR spectra was recorded on Agilent DD2 − 600 MHz spectrometer (Agilent, USA) at room temperature.

The FT-IR spectra of four pectin samples were recorded by using a Nicolet iN10 instrument (Thermo Fisher Scientific, USA) (Zhang et al., 2018). Samples (2 mg) were mixed with KBr powder and then pressed into pellets for FT-IR measurements in the range of 4000 − 400 cm^{-1}.

2.6. Atomic force microscopy (AFM)

Microstructures of pectic samples were acquired by AFM according to Zhang et al., 2018. Briefly, the pectic samples were dissolved in ultrapure water with a final concentration of 1 mg mL^{-1} under continuous stirring for 2 h and then, incubating at 80 °C for 2 h. Subsequently, the diluted pectin solutions (10 μg mL^{-1}) containing equal mass of sodium dodecyl sulfate (SDS) were stirred for 24 h to depolymerize the macromolecules. A 10 μL of sample solution was filtered through a 0.22 μm filter and dropped onto freshly cleaved mica

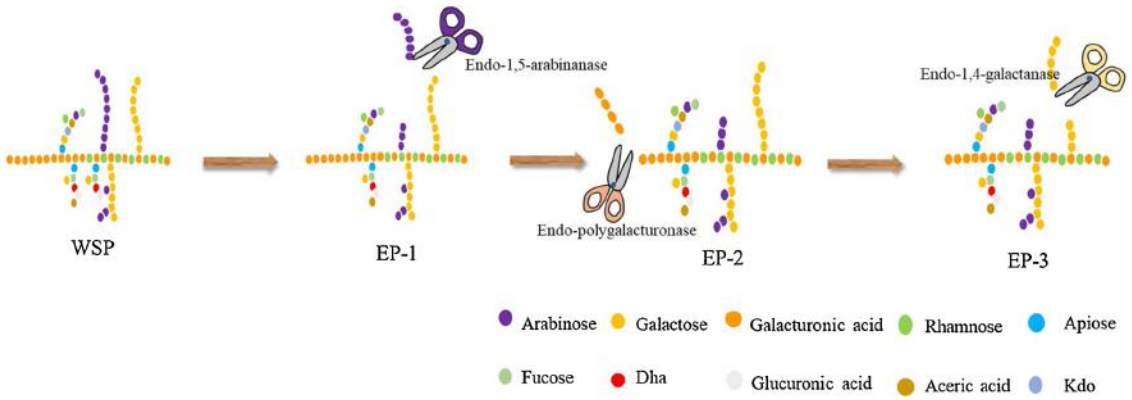

Fig. 1. The sequence for enzyme-modification.

substrate. Afterwards, the mica substrates were air-dried and then observed by AFM (XE-70, Park Scientific Instruments, Suwon, Korea), operated in a tapping mode at room temperature. The probe was a classical silicon cantilever (Si_3N_4) with a spring constant of 0.2 N/m and a resonance frequency of approximately 13 kHz. XEI data processing software was used for image manipulation.

2.7. Binding assay by surface plasmon resonance (SPR) assay

The SPR assay was performed following our previous method (Wei et al., 2019). Binding affinities of WSP and treated pectins to Gal-3 were performed on a BIAcore 3000 system (GE Healthcare, USA). Gal-3 protein was immobilized on an activated CM5 sensor chip (GE Healthcare, USA). Pectic samples were dispersed in HBS-EP buffer (0.01 M HEPES, 0.15 M NaCl, 3 mM EDTA, and 0.005 % surfactant P20, pH 7.4) and gradiently diluted to different concentrations. Each concentration of these sample was injected individually at a flow rate of 30 μL/min for 3 min, followed by dissociation and regeneration. Data analysis was performed through BIAcore 3000 evaluation software.

2.8. Anti-proliferation activity assay

Anti-proliferation activity was evaluated in MCF-7 (human breast cancer, cultured in DMEM with 10 % FBS) and A549 (human lung carcinoma, cultured in RPMI 1640 with 10 % FBS) cell lines. Both of the cells were incubated at 37 °C and 5% CO_2. Briefly, 100 μL of the cells were seeded in a 96-well plate at a concentration of 5×10^3/well. After 24 h of incubation, 100 μL of pectin sample solution at various concentration (2000 μg mL^{-1}, 1000 μg mL^{-1}, 500 μg mL^{-1}, 250 μg mL^{-1}, 125 μg mL^{-1}, 63 μg mL^{-1}) were slowly added to each well. MCP served as the positive control. After incubating for 48 h, 20 μL of methyl thiazolyl tetrazolium (MTT, 5 mg mL^{-1}) was added and the cells were further incubated for 4 h at 37 °C. After removing the medium, a volume of 150 μL dimethyl sulfoxide (DMSO) was added to each well to dissolve the resulting formazan. The absorbance was measured at 490 nm using a microplate reader (Bio-Rad, USA) and the anti-proliferation effect was calculated as

Anti-proliferation effect (% control) = $[1\text{-}(A_2 - A_0)/(A_1 - A_0)] \times 100$.

(A_0, A_1, A_2 respectively represent the absorbance of the system containing only medium, the absorbance of the system with cells, the absorbance of the system with pectin sample or MCP.)

2.9. Statistical analysis

All experiments were carried out in triplicate and the average of three independent experiments were used as the statistical result. The one-way analysis of variance (ANOVA) was conducted, followed by Duncan's multiple range test at significance level of 0.05 using SPSS software (version 19; IBM Corporation, New York, NY, USA).

3. Results and discussion

3.1. Molecular properties

The relative molecular information of WSP, EP-1, EP-2, EP-3 were revealed in Table 1, which were calculated using Astra 6.1. The weight average of molar mass (Mw) of these four samples were 5.93×10^5 g mol^{-1}, 5.26×10^5 g mol^{-1}, 4.72×10^5 g mol^{-1}, 3.70×10^5 g mol^{-1}, respectively. The molecular weight of WSP and these enzyme-modified pectins gradually decreased, but all of these samples had a molecular weight significantly larger than the Gal-3 protein. Enzymatic modification removed specific side chains and no remarkable changes in the average molecular weight was observed. Polydispersity coefficients (Mw/Mn) were 3.15, 5.79, 2.36, 2.10, respectively, which indicated

Table 1
Molecular and conformation parameters of WPS and enzyme-modified fractions.

Parameters	Samples			
	WSP	EP-1	EP-2	EP-3
Mn (g/mol)	$(1.88 \pm 0.03) \times 10^5$	$(0.91 \pm 0.01) \times 10^5$	$(2.00 \pm 0.03) \times 10^5$	$(1.76 \pm 0.01) \times 10^5$
Mp (g/mol)	$(1.62 \pm 0.02) \times 10^5$	$(0.41 \pm 0.01) \times 10^5$	$(1.46 \pm 0.03) \times 10^5$	$(1.05 \pm 0.03) \times 10^5$
Mw (g/mol)	$(5.93 \pm 0.02) \times 10^{5*}$a	$(5.26 \pm 0.08) \times 10^{5*}$a	$(4.72 \pm 0.01) \times 10^{5*}$b	$(3.70 \pm 0.06) \times 10^{5*}$c
Mw/Mn	3.15 ± 0.03b	5.79 ± 0.01c	2.36 ± 0.03a	2.10 ± 0.02a
Rh (nm)	0.449 ± 0.02a	0.576 ± 0.02a	0.635 ± 0.05a	0.654 ± 0.03a
[η] (mL/g)	10.788 ± 0.01	8.22 ± 0.01	12.612 ± 0.04	10.12 ± 0.03
K (mL/g)	$(4.22 \pm 0.04) \times 10^{-3}$	$(1.77 \pm 0.01) \times 10^{-3}$	$(1.18 \pm 0.04) \times 10^{-4}$	$(5.54 \pm 0.04) \times 10^{-4}$
α	0.72 ± 0.01a	0.77 ± 0.01a	0.98 ± 0.04a	0.83 ± 0.03a

Mn: number-average of molar mass; Mp: peak-average of molar mass; Mw; weight-average of molar mass; Rh: hydrodynamic radius. Means with the different letter are significantly different between columns ($p < 0.05$), *Significant against the Mw of Gal-3 (31 KDa) at $p < 0.05$.

Table 2
Monosaccharide compositions (mol%) of WSP, EP-1, EP-2, EP-3.

	Ara	Fuc	GalA	Gal	GlcA	Glc	Man	Rha	Rib	Xyl
WSP	48.83 ± 2.68c	5.53 ± 0.85b	24.96 ± 0.11a	11.80 ± 0.58a	0.20 ± 0.04a	0.61 ± 0.10a	0.30 ± 0.02a	4.16 ± 0.05a	0.49 ± 0.29a	2.09 ± 0.10a
EP-1	12.19 ± 0.02a	0.30 ± 0.01a	49.80 ± 0.01b	19.13 ± 0.00a	0.47 ± 0.00a	3.86 ± 0.01c	1.38 ± 0.03b	7.15 ± 0.01b	1.63 ± 0.02b	4.09 ± 0.03b
EP-2	17.78 ± 0.83a	0.13 ± 0.00a	26.47 ± 0.34a	28.58 ± 0.30b	0.70 ± 0.02a	4.27 ± 0.24c	1.63 ± 0.01b	10.92 ± 0.24c	1.50 ± 0.00b	7.73 ± 0.24c
EP-3	26.94 ± 1.03b	4.55 ± 0.52b	27.23 ± 2.64a	14.04 ± 1.32a	1.31 ± 0.47a	1.72 ± 0.03b	1.18 ± 0.02b	15.11 ± 0.53d	0.81 ± 0.03a	7.32 ± 0.02c

Ara: arabinose; Fuc: fucose; Man: mannose; GalA: galacturonic acid; Gal: galactose; GlcA: glucuronic acid; Glc: glucose; Rha; rhamnose; Rib: ribose; Xyl: xylose; Means with the different letter are significantly different between lines ($p < 0.05$).

that all of these pectin samples were polydisperse polysaccharide with wide molecular weight distribution. The relative information about chain conformation was able to further provide the spatial changes of sugar chains. The Mark-Houwink-Sakurada equation ($[\eta] = KM^{\alpha}$) is an important parameter to determine the chain conformation of macromolecules. The exponent (α) of Mark-Houwink-Sakurada equations for the samples were 0.72, 0.77, 0.98, 0.83 (Table 1) all falling in the 0.6–1.0 range corresponding to semi-flexible chains (Wang & Zhang, 2009). These results suggested that enzymatic treatment had no effect on the chain conformation.

3.2. Monosaccharide composition

Monosaccharide composition of these pectin samples were listed in Table 2. WSP contained approximately 50 % arabinose and these arabinan side chains wrapped around the pectin molecule, thus, blocking enzymatic cleavage by polygalacturonase and galactanase. Therefore, the arabinanase digestion was carried out first. After treatment of endo-1,5-α-arabinanase hydrolysis, the ratio of Ara residues in the pectin molecule reduced notably from 48.83 mol% to 12.19 mol%, suggesting that the arabinanase selectively removed three quarters of arabinan sidechains. The second step of endo-polygalacturonase hydrolysis seemed to remove nearly half of the galacturonic acid residues, which enriched the RG-I regions from 45.62 mol% in EP-1 to 68.2 % mol% in EP-2. EP-3 exhibited quite lower amount of galactose (14.04 mol%) as compared to EP-2 (28.58 mol%), indicating that endo-1,4-β-galactanase successfully hydrolyzed part of β-1,4-galactose sidechains.

All pectic polysaccharides primarily consisted of Rha, GalA, Gal, and Ara. The ratios of Rha/GalA in WSP, EP-1, EP-2, EP-3 were 0.17, 0.14, 0.41 and 0.55, respectively, all categorized as RG-I type (Rha/Gal ratio range from 0.05 to 1.0) (Zhang, Lan et al., 2016). The (Gal + Ara)/Rha ratio of these samples were 14.57, 4.38, 4.25, 2.71, corroborating that sugar side chains were gradually decreasing and the linearity of the samples were sequentially improved.

3.3. Structural characterization

The ^{1}H NMR spectra were recorded to further identify the changes of precise structure between these four samples. Detailed structural information about the proton environment were depicted in Fig. 2. Some assignments of 1H chemical shifts were listed in Table 3. All the four spectra corroborated the main structural features of RG-I pectin. The proton peak signals were mainly distributed at anomeric proton region (5.00–5.30 ppm) and the region of 3.70–4.70 ppm. In the anomeric region, some predominant peaks at 5.0–5.2 ppm were assigned to the H-1 of different types of arabinose (Zhang et al., 2018) and the signals around 5.30 ppm could be attributed to the H-1 of rhamnose (Li et al., 2019). In the ^{1}H spectra of WSP, some evident peaks attributed to the arabinose residue are exhibited. The high peaks at 5.11 ppm, 5.14 ppm and 5.18 ppm in anomeric protons region was derived from →5)-α-Ara-(1→, →3, 5)-α-Ara-(1→, →3)-α-Ara-(1→, respectively (Li et al., 2019), among which the signal at 5.11 ppm is the highest. The signal at 5.09 ppm was assigned to →4)-α-GalA-(1→ residue (Rosenbohm, Lundt, Christensen, & Young, 2003) and the signal at around 5.30 ppm correspond to the H1 of →2)-α-Rha-(1→ residue (Li et al., 2019). The short peaks around 4.7 ppm (4.69 ppm and 4.66 ppm) were attributed to H5 of GalA and H1 of β-1,4-Gal residues (Li et al., 2019). The assignment of other peak signals were annotated in Fig. 2. In the EP-1 spectrum, the signal peaks for Ara, such as peaks at 5.11 − 5.18 ppm, 4.46 ppm, 4.30 ppm and 4.15 ppm, were obviously less intense than those in WSP. Compared to that of EP-1, EP-2 spectrum exhibited markedly weaker signal of galacturonic acid at 5.10 ppm, 4.44 ppm (Zhi et al., 2017). Two obvious peaks at around 4.67 ppm and 4.64 ppm in EP-2 spectrum, which can be assigned to the H-1 of →4)-β-Gal-(1→ and →3)-β-Gal-(1→ residues, respectively, showed an evident decrease in the spectrum of EP-3, especially the signal assigned to H-1 of →4)-β-Gal-(1→. Therefore, 1H NMR spectra suggested that these enzymes had significant effect on debranching in WSP, which was consistent with the result of monosaccharide analysis.

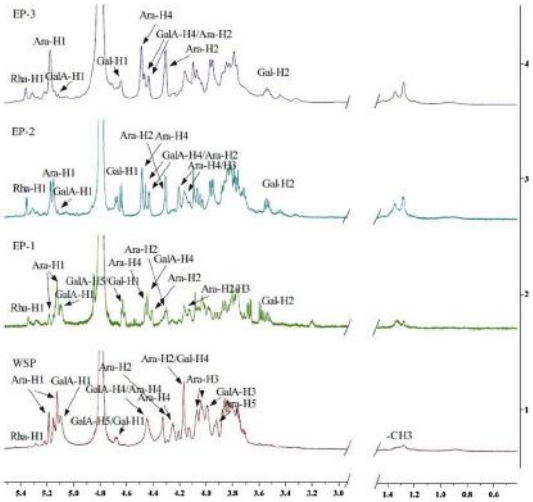

Fig. 2. The ^{1}H NMR spectra of WSP, EP-1, EP-2, EP-3.

The infrared spectra of the four samples were presented in Fig. 3. All of WSP and the enzyme-modified products displayed similar spectral bands as infrared spectroscopy is relatively insensitive to subtle changes in the structural analysis of macromolecules. The typical peaks at 3423 cm^{-1} were assigned to O—H stretching vibration in monosaccharide units, and the adsorption at 2933 cm^{-1} was attributed to the C–H stretching of CH_2 groups (Zhang et al., 2018). The degree of methyl esterification (DM) of pectin can be estimated according to peaks in the region between 1740 cm^{-1} and 1630 cm^{-1} (Chen et al., 2017; Fellah, Anjukandi, Waterland, & Williams, 2009). Usually, the COO-R groups have characteristic peak area around 1740 cm^{-1} and the 1630 cm^{-1} correspond to COO- of GalA in pectin (Gnanasambandam & Proctor, 2000; Ren et al., 2019). These results in FT-IR spectra showed that all of these pectin samples were almost non-esterified pectin due to these evident peaks at 1630 cm^{-1} and none at 1740 cm^{-1}. Also, as shown in Fig. 3, carboxylate group in GalA had symmetrical stretching band at 1415 cm^{-1}, confirming the presence of uronic acid in pectin (Saberian, Hamidi-Esfahani, Gavlighi, & Barzegar, 2017). After enzyme

Table 3
1H NMR chemical shifts assignments of WSP, EP-1, EP-2 and EP-3.

Residues	Samples			
	WSP	EP-1	EP-2	EP-3
→3)-α-Ara-(1→	5.18(H1);4.16(H2); 4.25(H4)	5.18(H1);4.15(H4)	5.18(H1)	5.21(H1)
→5)-α-Ara-(1→	5.11(H1);4.32(H2); 4.13(H3);4.20(H4); 4.92(H5)	5.12(H1);4.30(H2); 4.13(H3)	5.14(H1);4.30(H2); 4.19(H4)	5.16(H1); 4.30(H2)
→3,5)-α-Ara-(1→	5.14(H1);4.07(H3); 4.44(H4)	5.14(H1);4.41(H2); 4.15(H3);4.46(H4)	5.14(H1);4.43(H2); 4.16(H3);4.47(H4)	4.43(H2); 4.15(H3)
→4)-α-GalA-(1→	5.09(H1);3.99(H3); 4.44(H4);4.69(H5)	5.09(H1);4.44(H4)	5.11(H1);4.68(H5); 4.46(H4)	5.11(H1); 4.46(H4); 4.68(H5)
→3)-β-Gal-(1→	4.16(H3)	4.61(H1)	4.64(H1)	4.64(H1)
→4)-β-Gal-(1→	4.66(H1);4.44(H4)	4.63(H1);3.54(H2)	4.66(H1); 3.55(H2)	4.67(H1); 3.55(H2)

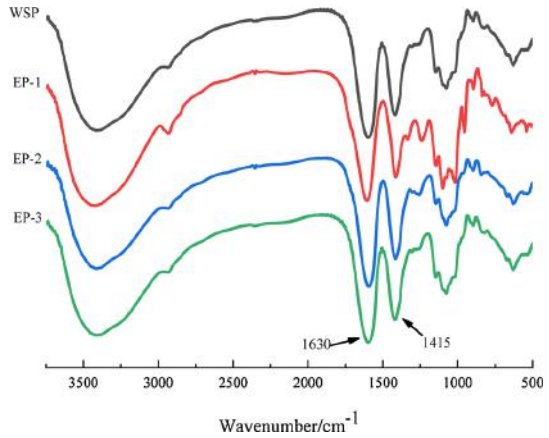

Fig. 3. IR spectra (% transmittance as a function wavenumber) of WSP, EP-1, EP-2, EP-3.

treatment, these treated pectin still exhibited low level of esterification, which indicated that enzymatic modification didn't change the esterification pattern. The wavenumbers between 1010 and 1150 cm^{-1} (*e.g.* 1024 cm^{-1}, 1076 cm^{-1}, 1145 cm^{-1}) corresponded to C—O and C—C vibration of glycosidic bonds and the pyranose (Li et al., 2019; Liu et al., 2016; Sucheta, Misra, & Yadav, 2020) and no changes caused by enzyme modification were found in these pyranose configuration.

3.4. Surface morphology

AFM technique was next employed to image the surface morphology of WSP, EP-1, EP-2 and EP-3 (Fig. 4). The long branching sugar chains could be observed in WSP, which might be the α-1.5-arabinan sidechains since WSP contained high amount of arabinose. After hydrolysis of endo-1,5-α-arabinanase, many short straight chains occurred, suggesting the notably decreasing in the amount of neutral sugar in EP-1. And then endo-polygalacturonase degraded the arborization-like structure, which made EP-2 appear to be short chains with many short branches, and the chain-chain interaction was more intensive in EP-2. It seemed that some HG regions were embedded in the trunk of RG-I and some existed as sidechain of RG-I. At last, the endo-1,4-β-galactanase resulted in significant sidechains depolymerization and EP-3 contains short backbone with very few branches. In addition, some irregular spherical conformation with the heights between 1 − 5 nm were observed within these molecule shapes, which implicated the existence of polymer. The loss of branching and homogalacturonan can reduce aggregated pectic complexes (Round, Rigby, MacDougall, & Morris, 2010), which could be observed in EP-2 image. Taken together, these AFM results were consistent with the semi-flexible chain conformation in SEC-MALLs analysis.

3.5. Binding affinity on Gal-3

The result of SPR analysis presented smooth binding curves between the samples and Gal-3 (Fig. 5). Gal-3 is a β-galactose-binding and tumor-related protein with key roles in accelerating cancer, fibrosis, carcinogenesis, and several other diseases. Therefore, the excellent anti-Gal-3 activity of RG-I pectin make it a non-toxic and effective inhibitory agent in disease therapy. Gal-3 inhibitors, such as MCP and ginseng pectin, have been reported to occupy the carbohydrate recognition domain (CRD) inside Gal-3 protein molecule *via* the galactan side chain (Gao et al., 2013; Zhang, Lan et al., 2016), which can explain the decrease of KD value between EP-2 and EP-3 (Table 4). Due to the effect of endo-1,4-β-galactanase, half of the galactan sidechains were removed in EP-2, which led up to approximately 3-fold decrease in the binding affinities. In addition, binding kinetics of WPS, EP-1 and EP-2 to Gal-3 were 0.321 μM, 0.48 μM, 0.56 μM, respectively, which suggested that partly removal of α-1,5-arabinan and HG region could impair the WSP's activity against Gal-3. Regarding to the results of SEC-MALLS analysis, all of the four molecular weights were between 3×10^5 and 6×10^5 g mol^{-1}, over 10-times larger than the molecular weight of Gal-3 (3.1×10^4 g mol^{-1}) (Fukumori et al., 2007). Compared to chemical modification, which decreases the Mw of pectin to 7.9×10^3 g mol^{-1}, enzyme digestion did not cause remarkable differences in molecular weight of the four samples, and no evident changes in the structural pattern were observed by FT-IR. Thus, the effects of different sidechains on the anti-Gal-3 activity could be assessed. Different domains inside Gal-3 can bind to different types of polysaccharides (Miller et al., 2016). For instance, the N-terminal (NT) tail of Gal-3 can bind to rhamnogalacturonan and F-face of CRD can interact with larger different polysaccharides (Miller et al., 2017). Therefore, the WSP might exert its arabinan sidechains to interact with the F-face in β-strands, which might account for the loss of activity caused by α-1,5-arabinanase (Gao et al., 2012). According to previous report, arabinose residues have positive or negative influence on the anti-Gal-3 activity due to different location (Gao et al., 2013) and α-1,5-arabinan exhibited negative effects, but the results in this study suggested that α-1,5-arabinan in the citrus RG-I also contributed to the activity, which may due to different length of sugar chains. In addition, the structure mode of RG-I backbone also make sense to the activity against Gal-3 (Zhang, Lan et al., 2016; Gao et al., 2013), so some HG segment is essential for WSP's activity, which is consistent with previous result (Maxwell et al., 2015). It has been reported that Gal/Ara ratio plays important role in binding Gal-3 (Gao et al., 2013). However, the ratio of Gal/Ara in WSP could not remarkably affect the anti-Gal-3 property. Compared to that of WSP (0.24), the Gal/Ara ratio of EP-1 increased to 1.56, but the binding affinity of WSP still decreased. Also, the importance of RG-I/HG ratio was not observed, though the RG-I and HG can work cooperatively. Conversely, more amount of neutral sugar sidechains might promote the anti-Gal-3 activity, since the decrease of binding affinity between pectin and Gal-3 was accompanied by a reduction in the degree of branching. In general, the SPR assay data suggested that all of the

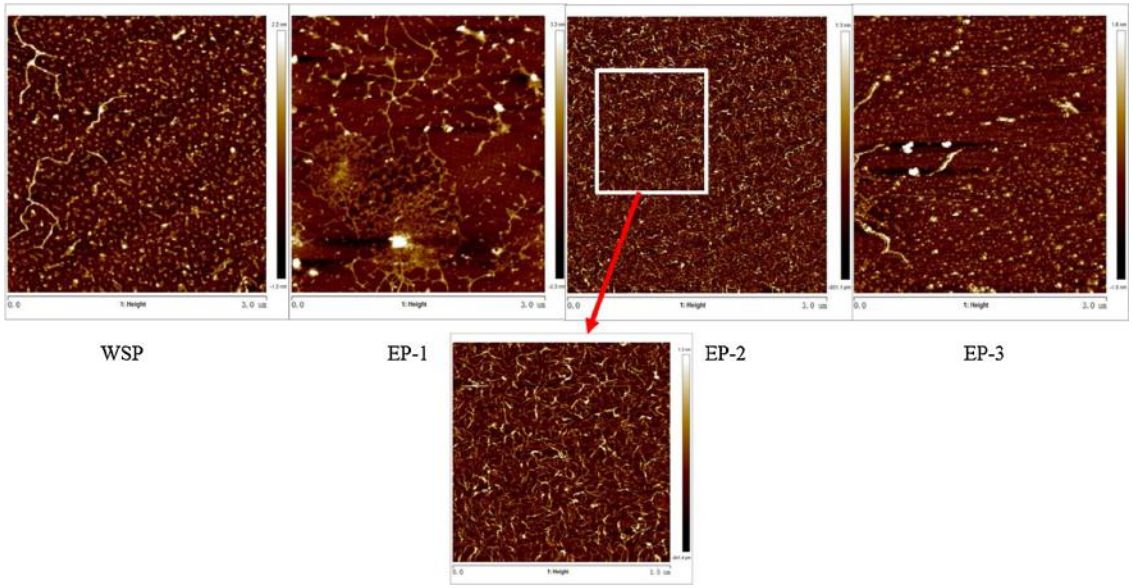

Fig. 4. Representative topographical AFM images of WSP, EP-1, EP-2, EP-3 (Each sample were at the concentration of 10 μg mL^{-1}).

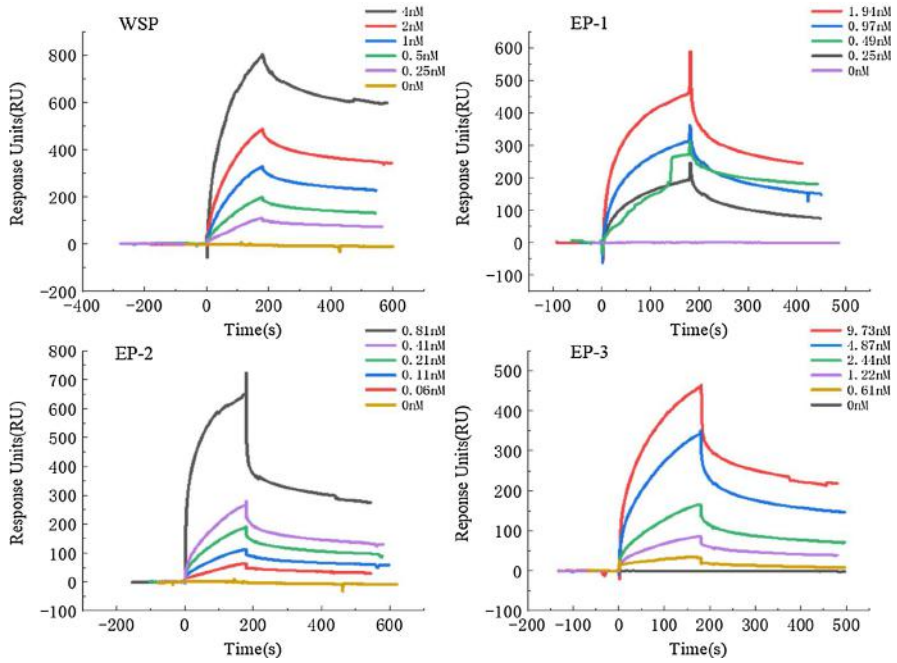

Fig. 5. SPR analysis of the binding affinities of WSP, EP-1, EP-2, EP-3 to galectin-3.

Table 4
The binding affinities of the four samples to galectin-3.

Samples	Mw (KDa)	ka (1/Ms)	kd (1/s)	KD(kd/ka) (μM)
WSP	593	1.86×10^{6}	5.98×10^{-4}	0.321
EP-1	526	5.34×10^{6}	2.56×10^{-3}	0.48
EP-2	472	2.20×10^{6}	1.23×10^{-3}	0.56
EP-3	370	7.85×10^{5}	1.52×10^{-3}	1.93

structural regions of WSP played an essential role in anti-Gal-3 activity, and the galactan sidechains possessed the largest effects. Moreover, WSP appeared to be a stronger Gal-3 inhibitor than most other polysaccharides (Gao et al., 2013; Wei et al., 2019; Zhao et al., 2017).

3.6. Anti-proliferation activities

One of the biological properties of Gal-3 is promoting the proliferation of cancer cells, therefore we employed MTT assay to determine the effects of WSP on Gal-3 function. The anti-proliferation activities of the four samples were tested on A549 (Fig. 4A) and MCF-7 (Fig. 4B) cell lines *in vitro* and MCP was employed as the positive control. As shown in Fig. 6, the proliferation of A549 and MCF-7 cell lines were evidently inhibited by all the samples in a dose-dependent manner. The IC_{20} values of the four samples against A549 were

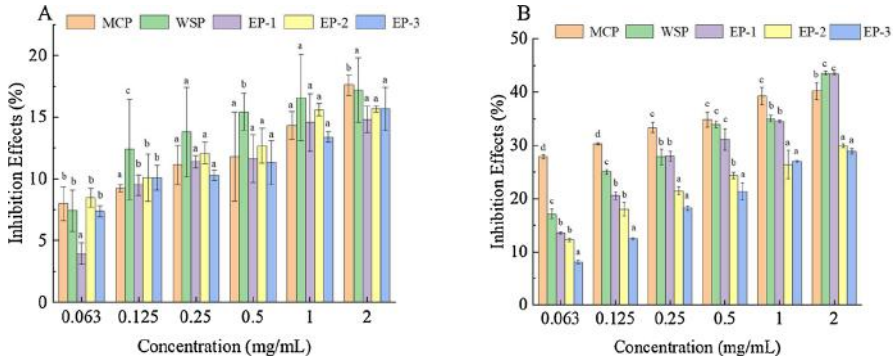

Fig. 6. Inhibition effects on A549 (A) and MCF-7 (B) cell lines viability. Means with the different letter are significantly different ($p < 0.05$), and error bars represent standard deviation.

0.12 mg mL^{-1}, 3.83 mg mL^{-1}, 11.19 mg mL^{-1}, 19.36 mg mL^{-1}, respectively. But in Fig. 6A, it seemed that no significant difference appeared among the groups treated with different samples, indicating that the anti-proliferation effects on A549 cells of these pectic fractions was not consistent with the anti-Gal-3 activity. The the IC_{30} values against MCF-7 were 0.33 mg mL^{-1}, 0.43 mg mL^{-1}, 1.84 mg mL^{-1}, 1.97 mg mL^{-1}, respectively. In addition, the four samples exhibited the remarkably inhibitory effects of WSP > EP-1 > EP-2 > EP-3 against MCF-7 cells, especially at the concentration of 0.125 mg mL^{-1}, which showed the same decreasing trend as the anti-Gal-3 activity. So MCF-7 was more sensitive to Gal-3 inhibitors, which may be owing to the higher expression level of Gal-3 compared to A549 (Wei et al., 2019). These data suggested that WSP and these debranched samples might exert the anti-tumor activity as a galactin-3 antagonist against cancer cells with high expression of Gal-3. Moreover, WSP even exhibited significantly stronger inhibitory effect than that of MCP at the concentration of 2 mg mL^{-1} in Fig. 6B, implicating the potential of WSP for curing cancers. Compared to other plant polysaccharides, the anti-proliferation activity of WSP against A549 cells was higher than the polysaccharides from *Flammulina velutipes* (Kom.) (Yang et al., 2012) and *Allium macrostemon Bunge* (Zhang, Wang, & Zeng, 2015), the inhibition effect against MCF-7 was stronger than an acidic polysaccharide from *Angelica sinensis (Oliv.) Diels* (Zhang, Zhou et al., 2016), indicating the potential antitumor activity.

4. Conclusions

The WSP recovered from canning processing water was determined to be RG-I type pectin with high amount of neutral sidechains, especially arabinan. Functionally, WSP exhibited very strong binding affinity with Gal-3, compared to most other polysaccharides. After partly removing the α-1,5-arabinan and β-1,4-galactan, the anti-Gal-3 activity of WSP decreased, indicating that besides the galactan sidechains, arabinan also contributed to the binding affinity between RG-I pectin and Gal-3 and long α-1,5-arabinan sidechains showed high activity. The total amount of neutral sidechains played an important role, not the ratio of Gal/Ara. In addition, our results suggested that RG-I and HG regions in WSP acted cooperatively, but the bioactivity of WSP was not significantly related to the ratio of RG-I/HG. This study provides some important information of the structure-function relationship of the citrus segment membrane pectin. These findings are also helpful in developing novel Gal-3 antagonists with low toxicity as well as the improved food additives in the industry.

CRediT authorship contribution statement

Dongmei Wu: Data curation, Formal analysis, Investigation, Project administration, Writing - original draft. **Jiaqi Zheng:** Software. **Weiwei Hu:** Supervision. **Xiaoliang Zheng:** Methodology. **Qiaojun He:** Resources. **Robert J. Linhardt:** Writing - review & editing. **Xingqian Ye:** Funding acquisition, Writing - review & editing. **Shiguo Chen:** Methodology, Funding acquisition, Writing - review & editing.

Declaration of Competing Interest

The authors declare that they have no conflict of interest.

Acknowledgments

This work was supported by National Natural Science foundation of China (31871815) and National Key Research and Development program of China (2017YFE0122300).

References

Chen, J., Cheng, H., Wu, D., Linhardt, R. J., Zhi, Z., Yan, L., et al. (2017). Green recovery of pectic polysaccharides from citrus canning processing water. *Journal of Cleaner Production, 144*, 459–469.

Fellah, A., Anjukandi, P., Waterland, M. R., & Williams, M. A. K. (2009). Determining the degree of methylesterification of pectin by ATR/FT-IR: Methodology optimization and comparison with theoretical calculations. *Carbohydrate Polymers, 78*, 847–853.

Gao, X., Zhi, Y., Zhang, T., Xue, H., Wang, X., Foday, A. D., et al. (2012). Analysis of the neutral polysaccharide fraction of MCP and its inhibitory activity on galectin-3. *Glycoconjugate Journal, 29*(4), 159–165.

Gao, X., Zhi, Y., Sun, L., Peng, X., Zhang, T., Xue, H., et al. (2013). The inhibitory effects of a rhamnogalacturonan I (RG-I) domain from ginseng pectin on galectin-3 and its structure-activity relationship. *The Journal of Biological Chemistry, 288*(47), 33953–33965.

Gnanasambandam, R., & Proctor, A. (2000). Determination of pectin degree of esterification by diffuse reflectance Fourier transform infrared spectroscopy. *Food Chemistry, 68*(3), 327–332.

Jiang, Y., & Du, J. (2017). Properties of high-methoxyl pectin extracted from “Fuji” apple pomace in China. *Journal of Food Process Engineering, 40*(3), e12497.

Jiang, X. N., Dang, Y. F., Gong, F. L., & Guo, X. L. (2019). Role and regulation mechanism of Gal-3 in non-small cell lung cancer and its potential clinical therapeutic significance. *Chemico-biological Interactions, 309*, 108724.

Khodaei, N., & Karboune, S. (2018). Optimization of enzymatic production of prebiotic galacto/galacto(arabino)-oligosaccharides and oligomers from potato rhamnogalacturonan I. *Carbohydrate Polymers, 181*, 1153–1159.

Laaf, D., Bojarova, P., Elling, L., & Kren, V. (2019). Galectin-carbohydrate interactions in biomedicine and biotechnology. *Trends in Biotechnology, 37*, 402–415.

Li, J., Li, S., Zheng, Y., Zhang, H., Chen, J., Yan, L., et al. (2019). Fast preparation of rhamnogalacturonan I enriched low molecular weight pectic polysaccharide by ultrasonically accelerated metal-free Fenton reaction. *Food Hydrocolloids, 95*, 551–561.

Liu, X. C., Zhu, Z. Y., Tang, Y. L., Wang, M. F., Wang, Z., Liu, A. J., et al. (2016). Structural properties of polysaccharides from cultivated fruit bodies andmycelium of Cordyceps militaris. *Carbohydrate Polymers, 142*, 63–72.

Liu, J., Zhao, Y., Wu, Q., John, A., Jiang, Y., Yang, J., et al. (2018). Structure characterisation of polysaccharides in vegetable "okra" and evaluation of hypoglycemic activity. *Food Chemistry, 242*, 211–216.

Mao, G., Wu, D., Wei, C., Tao, W., Ye, X., Linhardt, R. J., et al. (2020). Reconsidering conventional and innovative methods for pectin extraction from fruit and vegetable waste: Targeting Rhamnogalacturonan I. *Trends in Food Science & Technology* Advance online publication.

Maxwell, E. G., Belshaw, N. J., Waldron, K. W., & Morris, V. J. (2012). Pectin – An emerging new bioactive food polysaccharide. *Trends in Food Science & Technology, 24*,

64–73.
Maxwell, E. G., Colquhoun, I. J., Chau, H. K., Hotchkiss, A. T., Waldron, K. W., Morris, V. J., et al. (2015). Rhamnogalacturonan I containing homogalacturonan inhibits colon cancer cell proliferation by decreasing ICAM1 expression. *Carbohydrate Polymers, 132*, 546–553.
Miller, M. C., Ippel, H., Suylen, D., Klyosov, A. A., Traber, P. G., Hackeng, T., et al. (2016). Binding of polysaccharides to human galectin-3 at a noncanonical site in its carbohydrate recognition domain. *Glycobiology, 26*(1), 88–99.
Miller, M. C., Zheng, Y., Yan, J., Zhou, Y., Tai, G., & Mayo, K. H. (2017). Novel polysaccharide binding to the N-terminal tail of galectin-3 is likely modulated by proline isomerization. *Glycobiology, 27*(11), 1038–1051.
Mohnen, D. (2008). Pectin structure and biosynthesis. *Current Opinion in Plant Biology, 11*(3), 266–277.
Newlaczyl, A. U., & Yu, L. G. (2011). Galectin-3 - A jack-of-all-trades in cancer. *Cancer Letters, 313*, 123–128.
Nguyen, M. N., Ziemann, M., Kiriazis, H., Su, Y., Thomas, Z., Lu, Q., et al. (2018). Galectin-3 deficiency ameliorates fibrosis and remodelling in dilated cardiomyopathy mice with enhanced Mst1 signaling. *American journal of physiology-Heart and circulatory physiology, 316*, 45–60.
Oosterveld, A., Pol, I. E., Beldman, G., & Voragen, A. G. J. (2001). Isolation of feruloylated arabinans and rhamnogalacturonans from sugar beet pulp and their gel forming ability by oxidative cross-linking. *Carbohydrate Polymers, 44*, 9–17.
Pi, F., Liu, Z., Guo, X., Guo, X., & Meng, H. (2019). Chicory root pulp pectin as an emulsifier as compared to sugar beet pectin. Part 1: Influence of structure, concentration, counterion concentration. *Food Hydrocolloids, 89*, 792–801.
Rajput, V. K., MacKinnon, A., Mandal, S., Collins, P., Blanchard, H., Leffler, H., et al. (2016). A selective galactose-coumarin-Derived Galectin-3 inhibitor demonstrates involvement of Galectin-3-glycan interactions in a pulmonary fibrosis model. *Journal of Medicinal Chemistry, 59*(17), 8141–8147.
Ren, J. N., Hou, Y. Y., Fan, G., Zhang, L. L., Li, X., Yin, K., et al. (2019). Extraction of orange pectin based on the interaction between sodium caseinate and pectin. *Food Chemistry, 283*, 265–274.
Ridley, B. L., O'Neil, M. A., & Mohnen, D. (2001). Pectins: Structure, biosynthesis, and oligogalacturonide-related signalling. *Phytochemistry, 57*, 929–967.
Rosenbohm, C., Lundt, I., Christensen, T., & Young, N. G. (2003). Chemically methylated and reduced pectins: Preparation, characterisation by 1H NMR spectroscopy, enzymatic degradation, and gelling properties. *Carbohydrate Research, 338*(7), 637–649.
Round, A. N., Rigby, N. M., MacDougall, A. J., & Morris, V. J. (2010). A new view of pectin structure revealed by acid hydrolysis and atomic force microscopy. *Carbohydrate Research, 345*(4), 487–497.
Saberian, H., Hamidi-Esfahani, Z., Gavlighi, H. A., & Barzegar, M. (2017). Optimization of pectin extraction from orange juice waste assisted by ohmic heating. *Chemical Engineering and Processing Process Intensification, 117*(Supplement C), 154e161.
Sucheta, Misra, N. N., & Yadav, S. K. (2020). Extraction of pectin from black carrot pomace using intermittent microwave, ultrasound and conventional heating: Kinetics, characterization and process economics. *Food Hydrocolloids, 2020*(102), 105592.
Suthahar, N., Meijers, W. C., Sillje, H. H. W., Ho, J. E., Liu, F. T., & de Boer, R. A. (2018). Galectin-3 activation and inhibition in heart failure and cardiovascular disease: An update. *Theranostics, 8*(3), 593–609.
Voragen, A. G. J., Coenen, G. J., Verhoef, R. P., & Schols, H. A. (2009). Pectin, a versatile polysaccharide present in plant cell walls. *Structural Chemistry, 20*, 263–275.
Wang, J., & Zhang, L. (2009). Structure and chain conformation of five water-soluble derivatives of a β-d-glucan isolated from Ganoderma lucidum. *Carbohydrate Research, 344*, 105–112.
Wei, C., Zhang, Y., He, L., Cheng, J., Li, J., Tao, W., et al. (2019). Structural characterization and anti-proliferative activities of partially degraded polysaccharides from peach gum. *Carbohydrate Polymers, 203*, 193–202.
Wu, D., Zheng, J., Mao, G., Hu, W., Ye, X., Linhardt, R. J., et al. (2020). Rethinking the impact of RG-I mainly from fruits and vegetables on dietary health. *Critical Reviews in Food Science and Nutrition* Advance online publication.
Xue, H., Zhao, Z., Lin, Z., Geng, J., Guan, Y., Song, C., et al. (2019). Selective effects of ginseng pectins on galectin-3-mediated T cell activation and apoptosis. *Carbohydrate Polymers, 219*, 121–129.
Yan, L., Ye, X., Linhardt, R. J., Chen, J., Yu, D., Huang, R., et al. (2018). Full recovery of value-added compounds from citrus canning processing water. *Journal of Cleaner Production, 176*, 959–965.
Yang, W., Pei, F., Shi, Y., Zhao, L., Fang, Y., & Hu, Q. (2012). Purification, characterization and anti-proliferation activity of polysaccharides from Flammulina velutipes. *Carbohydrate Polymers, 88*(2), 474–480.
Yapo, B. M. (2011). Pectic substances: From simple pectic polysaccharides to complex pectins—A new hypothetical model. *Carbohydrate Polymers, 86*(2), 373–385.
Yapo, B. M., Lerouge, P., Thibault, J. F., & Ralet, M. C. (2007). Pectins from citrus peel cell walls contain homogalacturonans homogenous with respect to molar mass, rhamnogalacturonan I and rhamnogalacturonan II. *Carbohydrate Polymers, 69*(3), 426–435.
Yapo, B. M., Wathelet, B., & Paquot, M. (2007). Comparison of alcohol precipitation and membrane filtration effects on sugar beet pulp pectin chemical features and surface properties. *Food Hydrocolloids, 21*, 245–255.
Zhang, Z., Wang, F., & Zeng, X. (2015). The antitumor activity and neurotrophic activity of polysaccharides from Allium macrostemon bunge. *Food Research and Development, 36*(5), 107–115.
Zhang, H., Chen, J., Li, J., Yan, L., Li, S., Ye, X., et al. (2018). Extraction and characterization of RG-I enriched pectic polysaccharides from mandarin citrus peel. *Food Hydrocolloids, 79*, 579–586.
Zhang, T., Lan, Y., Zheng, Y., Liu, F., Zhao, D., Mayo, K. H., et al. (2016). Identification of the bioactive components from pH-modified citrus pectin and their inhibitory effects on galectin-3 function. *Food Hydrocolloids, 58*, 113–119.
Zhang, Y., Zhou, T., Wang, H. J., Cui, Z., Cheng, F., & Wang, K. P. (2016). Structural characterization and *in vitro* antitumor activity of an acidic polysaccharide from *Angelica sinensis* (Oliv.) Diels. *Carbohydrate Polymers, 147*, 401–408.
Zhao, J., Zhang, F., Liu, X., St Ange, K., Zhang, A., Li, Q., et al. (2017). Isolation of a lectin binding rhamnogalacturonan-I containing pectic polysaccharide from pumpkin. *Carbohydrate Polymers, 163*, 330–336.
Zheng, Y., & Mort, A. (2008). Isolation and structural characterization of a novel oligosaccharide from the rhamnogalacturonan of Gossypium hirsutum L. *Carbohydrate Research, 343*, 1041–1049.
Zhi, Z., Chen, J., Li, S., Wang, W., Huang, R., Liu, D., et al. (2017). Fast preparation of RG-I enriched ultra-low molecular weight pectin by an ultrasound accelerated Fenton process. *Scientific Reports of the Istituto Superiore Di Sanita, 7*, 1–11.